

## The dwarf nova EX Draconis: a short review

---

**Raymundo Baptista<sup>a,\*</sup> and Wagner Schlindwein<sup>a,b</sup>**

<sup>a</sup>*Departamento de Física, Universidade Federal de Santa Catarina - UFSC,  
Campus Trindade, Florianópolis, SC, Brazil*

<sup>b</sup>*Instituto Nacional de Pesquisas Espaciais - INPE,  
Avenida dos Astronautas, 1758, São José dos Campos-SP, Brazil*

*E-mail: [raybap@gmail.com](mailto:raybap@gmail.com), [wagner.schlindwein@astro.ufsc.br](mailto:wagner.schlindwein@astro.ufsc.br)*

EX Draconis (EX Dra) is a long period dwarf nova showing  $\approx 2$  mag outburst which lasts for  $\approx 7$  d and recur on a timescale of (20 – 30) d. Its deep eclipses allows one to trace the changes in surface brightness and radius of its accretion disk along the outburst cycle and to perform critical tests of the predictions of the thermal-viscous disk instability (DI) and the mass transfer outburst (MTO) models proposed to explain dwarf nova outbursts. The results of four critical tests are in clear contradiction with DI while in good agreement with MTO expectations. Furthermore, the observed variations in brightness and outer disk radius throughout EX Dra outbursts are well described by the response of a high-viscosity ( $\alpha = 3-4$ ) accretion disk to events in which the mass transfer rate increases by factors of  $\approx 30$  for  $\approx 7$  d, in line with MTO expectations. We further argue that the old expectation of accretion disk theory,  $\alpha \lesssim 1$ , seems unjustified and contradicts the values derived from dwarf nova outburst decline timescales if they are driven by MTO.

*The Golden Age of Cataclysmic Variables and Related Objects - VII (GOLDEN2025)  
1-6 September, 2025  
Mondello, Palermo, Italy*

---

\*Speaker

## 1. Context

Dwarf Novae (DN) are a sub-group of Cataclysmic Variables where a non-strongly magnetic ( $B \leq 10^5 G$ ) white dwarf (WD) accretes matter from a lower-mass, late-type donor companion (the secondary star) via an accretion disk. DN show recurrent outbursts at days-months timescales, in which the accretion disk increases in brightness by factors 20-100 during a few to several days [e.g., 44]. Two models were proposed in the 1970's to explain DN outbursts. In the thermal-viscous Disk Instability (DI) model [13, 19, 29, 36], matter accumulates in a cool, low-viscosity<sup>1</sup> and unsteady disk during quiescence ( $\alpha_c \sim 10^{-2}$ , viscous timescale longer than the outburst recurrence interval) and switches to a hot, higher viscosity regime ( $\alpha_h \sim 0.1-0.3$ ) during outbursts. In the Mass Transfer Outburst (MTO) model [7, 9, 37], the outburst is the viscous response of a disk with constant, high-viscosity ( $\alpha \sim 1-3$ , from the decline timescale of outbursting DN [e.g., 33, 44]) to a burst of enhanced mass transfer rate from the secondary star. Because of the permanent high-viscosity, the disk is expected to be in a steady-state both in outburst and in quiescence.

The widespread acceptance of DI as the correct explanation from the 1990's onwards was largely affected by a crucial misconception about the MTO, namely, that an enhanced mass transfer stream would necessarily stop at disk rim, leading to a significant increase in anisotropic emission from the bright spot (BS) at outburst onset as well as preventing MTO to trigger inside-out outbursts. The existence of inside-out outbursts and the lack of compelling evidence for the increase in BS luminosity at outburst onset were taken as strong evidence against MTO [44, and references therein]. However, numerical simulations of accretion disks show that when the gas stream is denser than the outer disk material (the likelihood of which increases with mass transfer rate [6]), the gas stream penetrates the disk and allows matter to be deposited in its inner regions [11, 12, 32], enabling inside-out outbursts while leaving no enhanced BS emission footprint at outburst onset. Having this in mind, the outcome of a MTO depends on the amplitude of the mass transfer enhancement,  $\Delta\dot{M}$  [8]. In low  $\Delta\dot{M}$  events, there is no room for significant gas stream penetration and the burst of matter is mostly deposited at disk rim, leading to outside-in outbursts with both an increase in BS luminosity and a transient shrinking of the disk at outburst onset (as a consequence of the large amount of gas of low angular momentum added to the outer disk regions [e.g., 31]) before the subsequent disk expansion. In high  $\Delta\dot{M}$  events, the gas stream penetrates the disk and may bring matter down to the circularization radius, leading to inside-out outbursts with no BS luminosity increase and no significant disk shrinking at outburst onset [37]. There is no room for gas stream penetration in the extremely low-viscosity ( $\alpha_c \approx 10^{-2}$ ) and high density quiescent disks expected in the DI framework [e.g., 6].

EX Dra is a relatively bright ( $V \approx 13.5$  mag), long-period ( $P_{\text{orb}} = 5.04$  h) and deeply eclipsing DN that shows  $\approx 2$  mag outbursts with a recurrence timescale of  $\approx (20-30)$  d [4, 14]. The trigonometric parallax distance estimate ( $241.2 \pm 1.3$  pc [17, 18]) is consistent with that derived through photometric parallax ( $290 \pm 80$  pc [4]). Measurements of the radial velocity of the secondary star, the emission lines (associated with the WD orbital movement), and the rotational broadening of the secondary star lead to a purely spectroscopic model for the binary [10, 15, 43], while the ingress/egress phases of the WD and of the BS lead to a purely photometric model of the binary

<sup>1</sup>here we adopt the prescription of Shakura & Sunyaev [40] for the accretion disk viscosity,  $\nu = \alpha c_s H$ , where  $\alpha$  is the non-dimensional viscosity parameter,  $c_s$  is the local sound speed and  $H$  is the disk vertical scaleheight.

[4, 39]. The photometric and spectroscopic models of the binary are consistent with each other within the uncertainties, indicating that the masses and radii of both stars, the orbital separation and orbital inclination are well constrained. Harrison et al. [23] derived a spectral type of K7 for the secondary star, while Harrison [22] fitted its near-infrared spectrum to obtain  $T_2 = 4000$  K, in agreement with the results of Shafter & Holland [39] and the CV evolutionary track of Knigge et al. [28], which predicts  $T_2 = 3800 \pm 200$  K.

The long orbital period (allowing eclipses to be sampled at a high phase resolution), relatively high brightness (ensuring high signal-to-noise light curves to be obtained), short outburst recurrence interval and deep eclipses (allowing the use of eclipse mapping techniques to trace the evolution of the disk surface brightness distribution along the outburst cycle [3, 25]) make EX Dra an ideal environment to test the predictions of the DN outburst models. The time-lapse eclipse mapping of EX Dra light curves throughout its outburst cycle [5, see Fig. 1] reveals the formation of a one-armed spiral structure in the disk at the early stages of the outburst (Fig. 1b) and that the disk expands during the rise phase until it fills most of the primary Roche lobe at maximum light (Fig. 1d). During the decline phase, the disk becomes progressively fainter (Fig. 1e) until only a small bright region around the WD is left at minimum light (Fig. 1f). Analysis of the radial brightness temperature distributions indicates that the disk appears to be in a steady-state during quiescence and at outburst maximum, but not during the intermediate stages. As a general trend, the mass accretion rate in the outer regions is larger than that in the inner disk in the ascending branch, while the opposite occurs during the descending branch. Fitting opaque steady disk models to radial temperature distributions allows one to estimate accretion rates of  $\dot{M} = 10^{-7.7 \pm 0.3} M_{\odot} \text{ yr}^{-1}$  ( $1.6_{-0.8}^{+1.6} \times 10^{18} \text{ g s}^{-1}$ ) at outburst maximum and  $\dot{M} = 10^{-9.1 \pm 0.3} M_{\odot} \text{ yr}^{-1}$  ( $5.0_{-2.5}^{+5.0} \times 10^{16} \text{ g s}^{-1}$ ) in quiescence [5].

Here we report critical tests of the predictions of the DI and MTO models against the EX Dra eclipse mapping results (Sect. 2), we show that the variations in brightness and disk radius throughout the EX Dra outburst can be well explained in the framework of the MTO model (Sect. 3), and we discuss the implications of our results in the context of DN outbursts and accretion disk theory (Sect. 4). The results are summarized in Sect. 5.

## 2. Testing outburst models with EX Dra eclipse mapping results

Observations of eclipsing dwarf novae throughout their outburst cycle provide a key opportunity to test the predictions and to discriminate between the DI and MTO explanations [2]. In particular, the critical tests are those the results of which are consistent with predictions of one of the models, but inconsistent with those of the other.

### 2.1 The quiescent disk

DI predicts that quiescent DN harbor low-viscosity ( $\alpha_c \leq 0.05$  [21]), unsteady accretion disks with a flat radial temperature distribution and a slow viscous response to eventual changes in mass transfer rate, while MTO predicts high-viscosity steady-state quiescent disks, with a fast response to changes in mass transfer rate. The differences in prediction are very significant. For EX Dra, the estimated viscous timescale of a quiescent DI disk is  $t_{\text{visc}}(\text{DI}) \geq 60$  d, which is much longer than its (20 – 30) d outburst recurrence time – indicating that there is not enough time to reach a state-state during quiescence [37]. However, the eclipse mapping analysis of Baptista & Catalán [5] shows

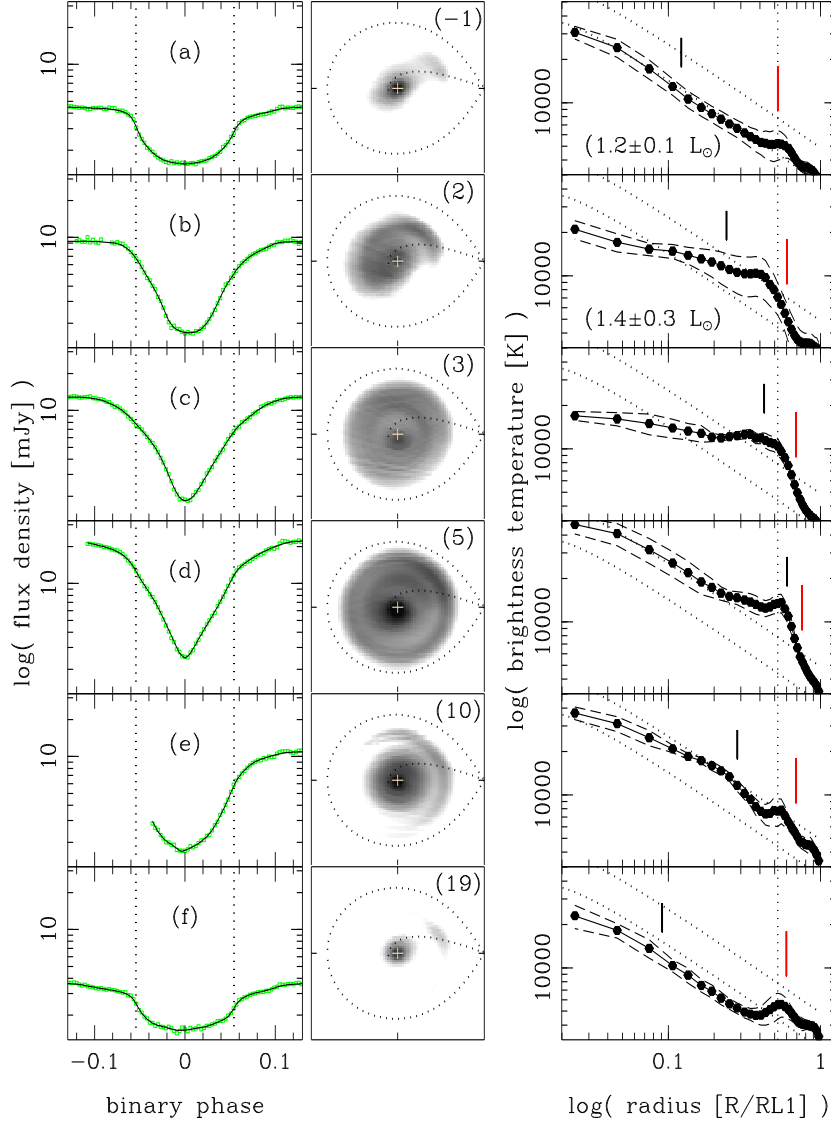


**Figure 1:** Time-lapse eclipse mapping of the dwarf nova EX Dra along its outburst cycle. Left-hand panels: Data (green dots) and model (solid line) light curves in (a) quiescent, (b) early rise, (c) late rise, (d) outburst maximum, (e) early decline, and (f) late decline stages. Vertical dotted lines mark ingress/egress phases of disk center. Middle panels: eclipse maps in a logarithmic grayscale; dark regions are brighter. Dotted lines show the primary Roche lobe and the ballistic trajectory of the gas from the secondary star; crosses mark the center of the disk. The secondary star is to the right of each panel; the stars and the accretion disk gas rotate counter-clockwise. The numbers in parenthesis indicate the time (in days) elapsed since outburst onset. Right-hand panels: azimuthally-averaged radial brightness temperature distributions for the eclipse maps in the middle panels. Dashed lines show the  $1\text{-}\sigma$  limit on the average temperature for a given radius. A dotted vertical line depicts the radial position of the BS in quiescence; vertical ticks mark the position of the outer edge of the disk (in red) and the radial position at which the disk temperature falls below 11000 K (blue). Steady-state disc models for mass accretion rates of  $\log M = -8.0$  and  $-9.0 M_{\odot} \text{ yr}^{-1}$  are plotted as dotted lines for comparison. Numbers in parenthesis list the integrated disk luminosity. From [5].

that both the radial temperature distribution at minimum light (Fig. 1f) and in quiescence (Fig. 1a) closely follow the  $T \propto R^{-3/4}$  law of opaque steady-state discs – respectively with mass accretion rates of  $\dot{M}(f) = (2.3 \pm 0.3) \times 10^{16} \text{ g s}^{-1}$  and  $\dot{M}(a) = (5.3 \pm 0.6) \times 10^{16} \text{ g s}^{-1}$  – and that the transition between these two steady-states occur in a viscous timescale of only  $t_{\text{visc}}(\text{quies}) = 1.5 \text{ d}$ , implying a quiescent viscosity parameter of  $\alpha \approx 2$ , in line with the high viscosity range inferred in Sect. 3. These results are in clear contradiction with DI while in good agreement with MTO expectations.

## 2.2 Accumulated mass versus accreted mass

In the DI framework, the maximum mass accumulated in the disk during quiescence,  $\Delta M_q(\text{max}) = \dot{M}_q \Delta t_q$  (derived under the assumption that all mass being transferred in quiescent is stored in the disk), is accreted onto the WD during outburst,  $\Delta M_o = \dot{M}_o \Delta t_o \leq \Delta M_q(\text{max})$ , at a predicted maximum outburst mass accretion rate of,

$$\dot{M}_o(\text{max}) = \frac{\Delta t_q}{\Delta t_o} \dot{M}_q, \quad (1)$$

where  $\Delta t_q$ ,  $\Delta t_o$  and  $\dot{M}_q$ ,  $\dot{M}_o$  are, respectively, the durations of the quiescence and of the outburst phases and the mass accretion rates in quiescence and in outburst. For EX Dra,  $\Delta t_q \approx (13 - 23) \text{ d}$ ,  $\Delta t_o \approx 7 \text{ d}$  [4], and one expects  $\dot{M}_o(\text{max}) \approx (2 - 3) \dot{M}_q \approx (1.0 - 1.5) \times 10^{17} \text{ g s}^{-1}$ . However, the inferred mass accretion rate at outburst maximum ( $1.6 \times 10^{18} \text{ g s}^{-1}$  [5]) is one order of magnitude larger than the DI prediction, implying that the mass accreted during outburst is also one order of magnitude larger than the maximum mass that could have accumulated in the disk during the previous quiescent phase. It is not possible to reconcile DI and the observations with such significant discrepancy, and one is lead to the conclusion that the outbursts of EX Dra must involve a significant increase in mass transfer rate during the outburst itself – in accordance with MTO expectations.

## 2.3 Enhanced stream emission at early rise

The early rise eclipse map (Fig. 1b) shows evidence of enhanced gas stream emission beyond impact at disk rim, suggesting the occurrence of gas stream overflow or penetration on that occasion (the reader is referred to Baptista & Schlindwein [6] for a comprehensive discussion on the possibilities of gas stream overflow and/or penetration in DN accretion disks). The upper panel of Fig. 2 compares the expected vertical scaleheight of EX Dra early rise DI and MTO ( $\alpha = 3$  and 4) disk models with the predicted vertical scaleheight of the gas stream for a secondary star of temperature  $T_2 = 3800 \pm 200 \text{ K}$  as a function of radius in units of the distance from WD to the inner lagrangian point L1. No stream overflow is possible at this outburst stage, as the disk scaleheights at disk rim ( $R_d = 0.6 R_{L1}$ ) are larger than the gas stream scaleheight at least at the  $3\text{-}\sigma$  confidence level. The lower panel of Fig. 2 compares the midplane densities of the EX Dra early rise DI and MTO disks models ( $\rho_d$ ) with the midplane density of the gas stream ( $\rho_s$ ), at disk rim, as a function of mass transfer rate. Stream penetration ( $\rho_s > \rho_d$ ) onto a DI disk might only occur at extremely large mass transfer rates,  $\dot{M}_2 > 10^{19} \text{ g s}^{-1}$ , far into the hot branch where the EX Dra accretion disk becomes stable against DI-driven outbursts – in marked contrast with its outbursting nature. On the other hand, stream penetration onto a MTO disk is much more plausible; it starts to occur at mass transfer rates slightly above the inferred quiescent mass transfer rate. Whereas the enhanced gas stream emission at early rise cannot be explained in the DI framework, it is the natural outcome

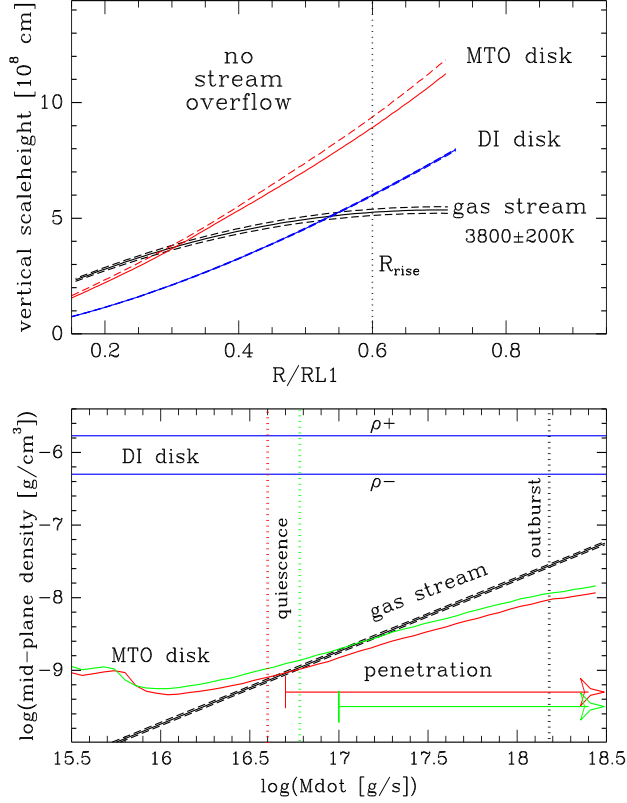


**Figure 2:** Top: Comparison of the vertical scaleheights of the disk and gas stream for EX Dra. Radial runs of the disk scaleheight are shown for DI (blue) and MTO (red, solid line for  $\alpha = 4$  and dashed line for  $\alpha = 3$ ) disk models. The vertical scaleheight of the gas stream is shown for  $T_2 = 3800 \pm 200$  K; dashed lines depict the corresponding  $1\text{-}\sigma$  limits. A vertical dotted line marks the outer disk radius at early rise,  $R_d = 0.6 R_{L1}$  [5]. Bottom: Disk and gas stream midplane densities as a function of mass transfer rate for a disk radius of  $R_d = 0.6 R_{L1}$ . The red (green) lines show the MTO disk midplane densities for  $\alpha = 4$  ( $\alpha = 3$ ), while blue lines show the range of possible DI disk midplane densities. Black lines show the gas stream midplane densities for  $T_2 = 3800 \pm 200$  K. Vertical dotted lines mark the inferred mass transfer rates in quiescence (in red for  $\alpha = 4$  and in green for  $\alpha = 3$ ) and in outburst.

of an increase in mass transfer rate onto a high-viscosity disk – as predicted for the EX Dra early outburst stage in the MTO framework.

## 2.4 Enhanced mass-transfer at early rise: cause or consequence?

The results of Sect. 2.3 are indicative of an enhanced mass transfer rate at this early outburst stage. The integrated disc luminosity at early rise ( $1.4 \pm 0.3 L_{\odot}$ , Fig. 1b) is comparable to that in quiescence ( $1.2 \pm 0.1 L_{\odot}$ , Fig. 1a) and is not enough to support the idea that the enhanced mass transfer rate could be triggered by an increased irradiation of the secondary star by the accretion disk. This led Baptista [2] to the conclusion that the observed enhanced mass transfer rate at early rise is not a consequence of the ongoing outburst, but its cause – suggesting that the outbursts of EX Dra are powered by events of enhanced mass transfer, as expected by MTO.

### 3. Mass-transfer outburst modelling

None of the critical tests performed in Sect. 2 is consistent with DI; all are in good agreement with MTO predictions. Given that the observational evidence largely favors MTO, we may ask the question: can MTO provide a satisfactory explanation of the disk radius and brightness changes throughout the EX Dra outburst?

Schlingwein & Baptista [37] developed an MTO code to simulate the response of an accretion disk to events of enhanced mass transfer, which includes a mass transfer event of smooth shape, mass deposition taking into account gas stream penetration<sup>2</sup>, and disc emission with either blackbody or gray atmosphere approximation. The smooth shape of the mass transfer event results in continuous changes in disk radius along the outburst and leads to a delay between the increase in  $\dot{M}$  in the outer regions and the accretion onto the WD, akin to the well known UV-delay effect seen in the initial outburst stages of several DN [e.g., 38]. Gas stream penetration allows for inside-out outbursts with minimal disk shrinkage at outburst onset, and gray atmospheres allow for optically thin outer disk regions.

This MTO simulation code was used to simultaneously model the observed variations in brightness at the  $V$ - and  $R$ -bands and in outer disk radius throughout the outburst cycle of EX Dra [37]. Observations made by amateur astronomers from AAVSO and VSNET were used to obtain a representative  $V$ -band light curve of EX Dra by combining measurements covering 14 outburst cycles, aligned according to the start of the rise to maximum. Only outbursts with amplitude and duration similar to those covered by the observations of Baptista & Catalán [5] were included. The data set was sliced in groups of 10 points and a median magnitude was computed for each group. The results are shown as blue symbols with error bars in the upper panel of Fig. 3. Red symbols indicate  $R$ -band out-of-eclipse magnitudes measured by Baptista & Catalán [5]. These are typical type B (inside-out) outbursts [42, 44], with comparable rise and decline timescales. The lower panel of Fig. 3 shows the evolution of the outer disk radius as measured by Baptista & Catalán [5]. There is no evidence of a decrease in outer disk radius at outburst onset.

A large grid of MTO models was built, covering a range of values for the 4 input parameters: quiescent mass transfer rate,  $\dot{M}_2^i$ , mass transfer rate at outburst maximum,  $\dot{M}_2^p$ , event duration,  $\Delta t_p$ , and viscosity parameter,  $\alpha$ . The value of  $\dot{M}_2^i$  is determined by the magnitude in quiescence, and that of  $\dot{M}_2^p$  is constrained by the magnitude during the plateau. The value of  $\Delta t_p$  is derived from the full-width-at-half-maximum of the outburst and the value of  $\alpha$  is defined by the outburst decline timescale. The best fit outburst model to the observations was found by calculating the  $\chi^2$  of the fit for each grid model. Solid lines in Fig. 3 show the best-fit model for the case of gray atmosphere local emission. The MTO model predicts significant gas stream penetration during outburst (red dashed line in the lower panel of Fig. 3), which eliminates the marked initial reduction in disk radius predicted by the simulations of Livio & Verbunt [31] and Ichikawa & Osaki [26] and leads to an outer disk radius variation consistent with the EX Dra observations.

The observed variations in brightness and outer disk radius throughout the outbursts of EX Dra are well described ( $\chi^2 \simeq 1$ ) by the response of a high-viscosity accretion disk to an event of enhanced mass transfer rate, in accordance with MTO predictions. The best-fit MTO models indicate viscosity

<sup>2</sup>The gas stream penetration radius ( $R_p$ ) is taken as the radius where the midplane gas stream density equals the midplane disk density. There is gas stream penetration when  $R_p < R_d$  [6].

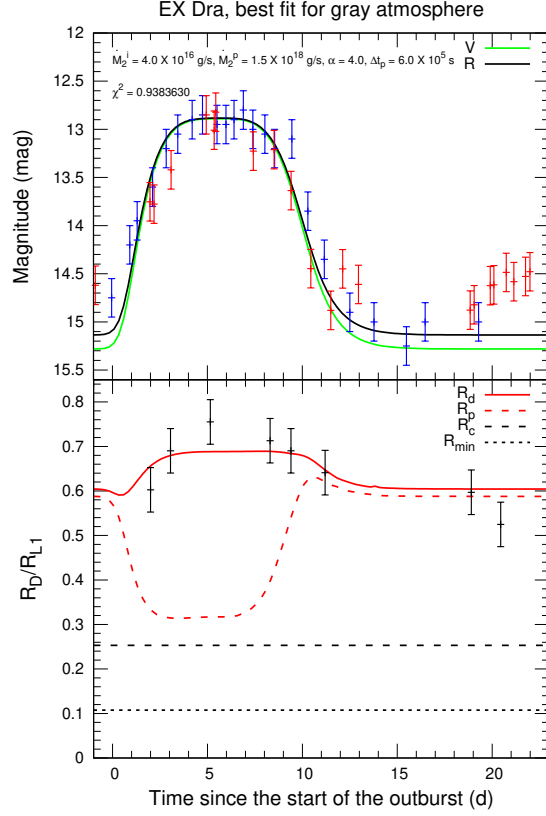


**Figure 3:** Top: Average V- (blue points) and R-band (red points) EX Dra outburst light curves with respect to the time since outburst onset, together with corresponding best-fit MTO model light curves for gray atmosphere local emission. The input parameters for this model are listed together with the  $\chi^2$  value of the fit. Bottom: Changes in disk radius as a function of time from outburst onset. The disk radius measurements by [5] are shown as points with error bars in comparison to the MTO model outer disk radius (solid red line) and the stream penetration radius (dashed red line). Black dashed and dotted lines depict the circularization radius and the radius of shortest stream distance from the WD, respectively.

parameters in the range  $\alpha = 3$  (blackbody local emission) to  $\alpha = 4$  (gray atmosphere local emission) and a mass transfer event of width  $\Delta t_p = 6 \times 10^5$  s  $\simeq$  7 d. The values of the quiescence and outburst maximum mass transfer rates inferred from the MTO model are consistent with those derived by Baptista & Catalán [5] at the  $1-\sigma$  limit [37].

#### 4. Is alpha larger than unity unphysical?

In their effort to overcome the absence of a theory of viscosity in differentially rotating fluid disks, Shakura & Sunyaev [40, 41] parametrized the kinematic viscosity in terms of the known quantities  $c_s$  and  $H$ , and transferred the ignorance on the unknown viscosity mechanism to the non-dimensional  $\alpha$  parameter,

$$\alpha = \frac{v_t l_t}{c_s H} + \frac{B^2}{4\pi \rho c_s^2}, \quad (2)$$



where  $v_t$  and  $l_t$  are respectively the turbulent velocity and the turbulent mixing length (in case of hydrodynamic turbulence),  $B^2/8\pi$  is the energy density of the chaotic magnetic field and  $\rho c_s^2/2$  is the thermal energy density of the matter in the disk (in case of magneto-hydrodynamic turbulence [e.g., 1, 24]). The theoretical expectation  $\alpha \lesssim 1$  is based on the assumptions that (i) the turbulent mixing length can not exceed the disk vertical scaleheight ( $l_t \leq H$ ) and (ii) the turbulence must be subsonic ( $v_t \lesssim c_s$ ) otherwise the turbulent motions would probably be thermalized by shocks [16, 40].

Frank et al. [16] noted that  $v_t > c_s$  could occur in disk regions where some physical input continually feeds a supersonic turbulence. Martin et al. [34] remarked that both the disk mass inflow and the rate of heating by viscous dissipation depend linearly on the value of  $\alpha$  and that, while a larger  $\alpha$  leads to a larger amount of energy dissipation (presumably through shocks), it also leads to a larger accretion rate which can provide the necessary larger energy to be dissipated. Hence, they concluded that the  $v_t \lesssim c_s$  assumption is not justified on energy arguments. In addition, Schlindwein & Baptista [37] argue that there is no reason to exclude the possibility that shocks in trans-sonic or supersonic turbulence may just provide the dissipative process required for viscous heating in accretion disks.

The  $l_t \leq H$  assumption is based on the idea that turbulence is isotropic. However, in an accretion disk angular momentum exchange occur in the radial direction, strong stretching of turbulent eddies or magnetic field lines occur in the azimuthal direction, and most of the energy resulting from viscous dissipation is transported in the vertical direction. It makes not much sense to believe that (hydrodynamical or magneto-hydrodynamical) turbulence in such an anisotropic environment should be isotropic [37]. Indeed, numerical simulations of the magneto-rotational instability show how an initially isotropic magnetic field rapidly becomes chaotic, anisotropic and significantly stretched in the radial direction, with the amount of field stretching being limited mostly by the radial width of the shearing box [24, see their Fig. 9]. In addition, the radial stretching of the magnetic field lines allows exchange of angular momentum over radial distances which greatly exceed the linear wavelength of the instability (which will be present as long as the minimum unstable wavelength do not exceed the disc thickness), thus indicating that  $l_t > H$ .

Given that both  $l_t > H$  and  $v_t > c_s$  are valid possibilities, the theoretical expectation  $\alpha \lesssim 1$  seems unjustified and there is no *a priori* reason to consider that  $\alpha > 1$  is unphysical [37].

Since the definition of  $\alpha$  in Eq. 2 is independent of both the isotropic and the subsonic assumptions, the parametrization of Shakura & Sunyaev [40, 41] is still applicable if these two assumptions are dropped. In the case of magneto-hydrodynamic turbulence, we may define the components of the Alfvén velocity as  $v_{Ai}^2 = B_i^2/4\pi\rho$ . For an anisotropic magnetic field, it is possible (and likely [24]) to have  $v_{A\phi}^2, v_{AR}^2 > c_s^2 > v_{Az}^2$  and, therefore,  $\alpha = v_A^2/c_s^2 > 1$ . Similarly, in the case of anisotropic hydrodynamic turbulence, the turbulent mixing length is allowed to be different for each direction,  $l_\phi \neq l_R \neq l_z$  (from the dynamics of an accretion disk one might expect  $l_\phi > l_R > l_z$ ). Therefore, it is possible (and likely) to have  $l_\phi, l_R > H > l_z$  and  $\alpha > 1$  as well, even in the case of subsonic turbulence. The accretion disk theoreticians are encouraged to explore this still untouched domain.

## 5. Summary

This short review of EX Dra can be summarized as follows:

- EX Dra is an eclipsing version of SS Cyg (the *bona fide* long-period DN), a gift provided by nature to allow us to test the current theories about DN outbursts.
- Time-lapse eclipse mapping of EX Dra throughout its outburst allow us to perform four critical tests of the DN outburst theories. The results of all four tests are in clear contradiction with DI while in good agreement with MTO expectations.
- The observed variations in brightness and outer disk radius throughout EX Dra outbursts are well described ( $\chi^2 \simeq 1$ ) by the response of a high-viscosity ( $\alpha = 3 - 4$ ) accretion disk to events in which the mass transfer rate increases by factors of  $\simeq 30$  for  $\simeq 7$  d, in line with MTO expectations.
- EX Dra is no anomaly; it teams with V2051 Oph, HT Cas, V4140 Sgr, EX Hya, YZLMi, and possibly SS Cyg and OY Car in an increasing group of DN the outbursts of which seems to be powered by MTO instead of by DI.
- There is no physical support for the assumptions that (i) the turbulent mixing length has to be lower than the disk vertical scaleheight and (ii) turbulence must be subsonic. The theoretical expectation  $\alpha \lesssim 1$  is unjustified.
- If outbursts in DN and soft x-ray transients are viscous events (instead of thermal-viscous instability events), than the viscosity parameters inferred from their outburst decline timescales are systematically larger than unity and the theoretical expectation  $\alpha \lesssim 1$  is inconsistent with observations.

## Acknowledgments

R. Baptista acknowledges financial support from CNPq grant 421034/2023-8. This study was financed in part by the Coordenação de Aperfeiçoamento de Pessoal de Nível Superior - Brasil (CAPES) - Finance Code 001.

## References

- [1] Balbus S. A., Hawley J. F., 1991, ApJ, 376, 214
- [2] Baptista R., 2012, Mem. Soc. Astr. It., 75, 282
- [3] Baptista R., 2016, in Astronomy at High Angular Resolution, Astroph. and Space Science Library, eds. H.M.J. Boffin, G. Hussain, J.-P. Berger, L. Schmidtbreick (Springer: Switzerland), p. 155
- [4] Baptista R., Catalán M. S., & Costa L., 2000, MNRAS, 316, 529
- [5] Baptista R., & Catalán M. S., 2001, MNRAS, 324, 599
- [6] Baptista R., Schlindwein W., 2022, AJ, 163, 108
- [7] Bath G. T., 1975, MNRAS, 171, 311

- [8] Bath G. T., Edwards A. C., & Mantle V. J., 1983, MNRAS, 205, 171
- [9] Bath G. T. & Pringle J. E., 1981, MNRAS, 194, 967
- [10] Billington I., Marsh T. R., & Dhillon V. S. 1996, MNRAS, 278, 673
- [11] Bisikalo D. V., Boyarchuk A. A., Chechetkin V. M., Kuznetsov O.A. & Molteni D., 1998, MNRAS, 300, 39
- [12] Bisikalo D. V., 2005, APS&S, 296, 391
- [13] Cannizzo J., 1993, in *Accretion Disks in Compact Stellar Systems*, ed. J. C. Wheeler (Singapore: World Sci. Publ. Co.), p. 6
- [14] Court J. M. C., Scaringi S., Littlefield C., et al. 2020, MNRAS, 494, 4656
- [15] Fiedler H., Barwig H., & Mantel K. H. 1997, A&A, 327, 173
- [16] Frank J., King A., & Raine D., 2002, *Accretion Power in Astrophysics - 3rd. edition*, (Cambridge: Cambridge Univ. Press)
- [17] Gaia Collaboration, Prusti T., de Bruijne J. H. J. et al., 2016, A&A, 595, A1
- [18] Gaia Collaboration, Vallenari A., Brown A. G. A., et al. 2023, A&A, 674, A1
- [19] Hameury, J. M. 2020, *Advances in Space Research*, 66, 1004
- [20] Hameury J. M., & Lasota J. P., 2014, A&A, 569, A48
- [21] Hameury J.-M., Menou K., Dubus G., Lasota J. P., Húre J.-M., 1998, MNRAS, 298, 1048
- [22] Harrison T. E. 2016, ApJ, 833, 14
- [23] Harrison T. E., Osborne H. L., & Howell S. B. 2004, AJ, 127, 3493
- [24] Hawley J. F., Balbus S. A., 1991, ApJ, 376, 223
- [25] Horne K. 1985, MNRAS, 213, 129
- [26] Ichikawa S., & Osaki Y. 1992, PASJ, 44, 15
- [27] King A., & Cannizzo J., 1998, ApJ, 499, 348
- [28] Knigge C., Baraffe I., & Patterson J., 2011, ApJS, 194, 28
- [29] Lasota J. P., 2001, *New Astronomy Review*, 45, 449
- [30] Livio M., & Pringle J. E. 1994, ApJ, 427, 956
- [31] Livio M., & Verbunt F. 1988, MNRAS, 232, 1P
- [32] Makita M., Miyawaki K., & Matsuda T., 2000, MNRAS, 316, 906

- [33] Mantle V. J. & Bath G. T., 1983, MNRAS, 202, 151
- [34] Martin R. G., Nixon C. J., Pringle J. E., Livio M., 2019, New Astron., 70,7
- [35] Menou K., Hameury J.-M., & Stehle R. 1999, MNRAS, 305, 79
- [36] Osaki Y, 1974, PASJ, 26, 429
- [37] Schlindwein W. & Baptista R., 2024, ApJ, 975, 92
- [38] Schreiber M. R., Hameury J.-M., & Lasota J.-P., 2005, in Proc. ASP Conf. 330, The Astrophysics of Cataclysmic Variables and Related Objects, ed. J.-M. Hameury & J.-P. Lasota (San Francisco, CA: ASP)
- [39] Shafter A. W., & Holland J. N. 2003, PASP, 115, 1105
- [40] Shakura N. I. & Sunyaev R. A., 1973, A&A, 24, 337
- [41] Shakura N. I. & Sunyaev R. A., 1976, MNRAS, 175, 613
- [42] Smak J. 1984, Acta Astron., 34, 161
- [43] Smith D. A., & Dhillon V. S. 1998, MNRAS, 301, 767
- [44] Warner B., 2003, Cataclysmic Variable Stars, Cambridge Astrophysics Series 28, (Cambridge: Cambridge University Press)

## DISCUSSION

**ALLEN SHAFTER:** What instability in the secondary star results in the modified mass transfer?

**RAYMUNDO BAPTISTA:** The original idea of an instability in the atmosphere of the secondary star [7, 9] was abandoned a long time ago. Currently, the most promising explanation for the sudden changes in mass transfer rate required by MTO involves starspots moving in and out of the inner lagrangian point L1. Livio & Pringle [30] and King & Cannizzo [27] pointed out that the passage of starspots in front of L1 can significantly reduce  $\dot{M}_2$ , leading Hameury & Lasota [20] to suggest that events of enhanced mass transfer may occur when there are no starspots transiting L1.